Article

Not peer-reviewed version

Green Synthesis Photoluminescent of Carbon Dots Extracted from Black Mulberry Fruits for Photocatalytic Degradation of Pollutant

H.F. Etefa * and FB Dejene

Posted Date: 24 May 2024

doi: 10.20944/preprints202405.1578.v1

Keywords: C-dots; Photodegradation; Black mulberry fruits; Photoluminescence; Pollutant

Article

Green Synthesis Photoluminescent of Carbon Dots Extracted from Black Mulberry Fruits for Photocatalytic Degradation of Pollutant

H.F. Etefa [1,*] and F.B. Dejene [2]

[1] Department of Physics, Walter Sisulu University, Mthatha 5117, South Africa
* Correspondence: hetefa@wsu.ac.za

Abstract: Biosynthesis of C-dots using black mulberry fruit as a precursor for C-dot synthesis is a novel approach. We successfully synthesized C-dots from the fruit extract by employing a hydrothermal autoclave. This green synthesis method offers a sustainable and environmentally friendly route for C-dot production. Our results demonstrate the efficient degradation of pollutants under visible light irradiation, indicating the strong photocatalytic activity of the C-dots. This finding has implications for environmental remediation and the elimination of harmful substances, showcasing the potential practical applications of C-dots in addressing water contamination issues. We made an effort to identify the optimum doping concentration of C-dots, and found that 0.2 mol% was the sweet spot. At this concentration, the photodegradation of pollutants reached an impressive 95.8%. The enhanced photocatalytic activity can be attributed to increased electron trapping due to more surface sites and different absorption wavelengths.. This work contributes to the synthesis of carbon dots using black mulberry fruits as a sustainable precursor, as well as the comprehensive analysis of their optical and photocatalytic properties.

Keywords: C-dots; Photodegradation; Black mulberry fruits; Photoluminescence; Pollutant

1. Introduction

Photoluminescent Carbon dots (C-dots) are nanoscale carbon-based materials with unique optical properties [1,2]. These dots exhibit photoluminescence, which means they can absorb light energy and re-emit it at a different wavelength[3]. The emission of light by these carbon dots is used for various applications, including sensing, imaging, and optoelectronics[4,5]. Black mulberry Fruits (Morus nigra) is a type of fruit that belongs to the Moraceae family[6,7]. In this research, carbon dots are derived from black mulberry fruits, implying that the researchers extracted and synthesized carbon dots from the fruit's components[8,9]. Photocatalytic degradation involves the use of a photocatalyst to break down or decompose organic pollutants in the presence of light[10]. The carbon dots derived from black mulberry fruits are investigated for their ability to act as a photocatalyst, facilitating the degradation of organic contaminants [11]. The utilization of waste effluents from Pollutant industries, as well as the application of Pollutant and fertilizers in agriculture, has resulted in elevated levels of organic pollutants in natural water bodies [12,13]. This influx of pollutants poses a potential risk as it can lead to the formation of carcinogenic intermediates, which have the potential to cause cancerous effects [14]. Nanostructures made of carbon with sizes under 5 nm are called "carbon dots." Since their discovery, they have drawn a lot of interest from materials science being a potential replacement for semiconductor quantum dots, particularly in biological applications owing to its low toxicity. Photocatalysis, solar power, bioimaging, and medication delivery are a few of their uses [15–17].

Due to worries about their toxicity to humans and persistence in ecosystems, a number of countries currently forbid the use of some Pollutant [18]. Because of its outstanding biocompatibility, optical qualities, non-toxic precursors, high aqueous solubility, and simplicity of surface passivation, photocatalytic degradation employing C-dots is essential for water purification and photon degradation[19,20]. Depending on the active ingredient, the procedure time for removing and

 doi:10.20944/preprints202405.1578.v1

mineralizing pollutant from water varies[21]. The application of innovative techniques for preparing such carbon dots with desired size, shape, and functionalities remains the key to the success in the theoretical chemistry fields and applied physics for nanomaterials applications and treatment of waste-water through photocatalytic degradation is very significant for the community because c-dots prepared from bluck mulberry fruits cheap, simple and available. Carbon quantum dots, ultrafine carbon nanomaterials below 5 nm, have gained attention for their excellent mechanical, chemical, and fluorescent capabilities, photostability, and biocompatibility [22–24]. With straightforward, affordable preparation methods offering a distinct advantage in nanotechnology, CDs are ideal for a variety of functions and have great photostability, biological compatibility, biosensing, and low cytotoxicity[25].The study needs a carbon dot synthesis method that is dependable, inexpensive, and rapid, differentiating top-down from bottom-up approaches based on the original carbon source[26]. Numerous Fluorescent C-dots derived from food wastes have a wide range of applications, such as sensing, drug delivery, gene transfer, biological imaging, and food safety. Examples of food wastes used for C-dots synthesis include banana peels, mango peels, sugarcane bagasse, Trapa bispinosa peels, bread, and wet olive pomace [27,28]. Due to their sustainability and favorable effects on the environment, the development of nanoscale photocatalysts with higher efficiency is attracting interest. Pollutant have been treated with C-dots, and wastewater has been treated with photocatalytic carbon dot hydrogels made from brewing waste [21,29,30]. This work significantly contributes to the field of carbon dots synthesis, characterization, and their application in photocatalysis, particularly in the context of pollutant degradation. The use of black mulberry fruits as a sustainable precursor for C-dot synthesis is a novel and eco-friendly approach. By utilizing a green synthesis method, we have demonstrated the potential for sustainable production of C-dots.This information is crucial for optimizing their performance in various applications.

2. Experimental Methods and Chemicals

2.1. Extraction of Black Mulberry Fruits

Distilled water, Ethylenediamine, aqueous solution, dichloromethane. Black mulberry fruits will be collected freshly from Umthatha. South Africa. It is first wash in water and the juice like blue color of the black mulberry will be collected and then filtered using 0.2 µm cellulose acetate membranes (filter paper).

2.2. Green Synthesis of C-Dots

A mixture of (40 ml) of freshly filtered black mulberry fruit liquid and 4 ml of ethylenediamine (EDA) will be placed in a 60 ml hydrothermal autoclave and heated to 200 °C for three hours. The freshly made black paste will be allowed to cool to room temperature before being centrifuged with DI water at 3000 rpm for 15 minutes to separate the insoluble components. To eliminate unreacted organic molecules, dichloromethane will next be added to the brown solution of C-dotss and centrifuged once more for 20 minutes at 3000 rpm. To eliminate larger sized particles, the upper aqueous layer will then be separated and centrifuged at 6,000 rpm for 20 min. The result will be a brownish-yellow supernatant. In order to characterize and use the prepared C-dotss, they will be kept at 4 °C [31,32] seen in **Figure 1** below.

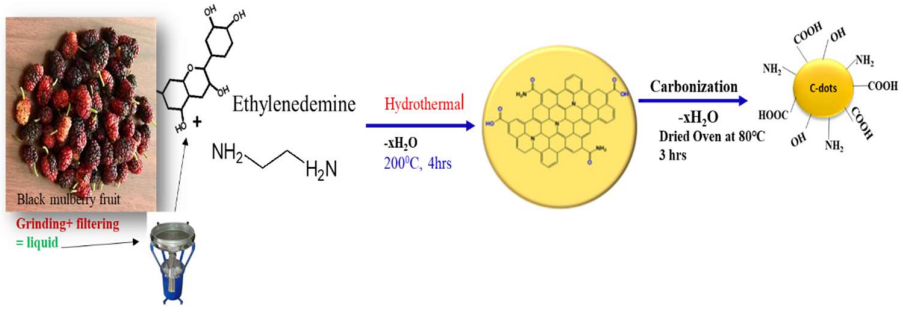

Figure 1. Green synthesis of Carbon dots extracted from black mulberry fruits.

 doi:10.20944/preprints202405.1578.v1

First, 2ml of deionized water and contaminated water will be measured separately using Uv-Visible and comparing absorption band. Similarly, dissolving 2ml of prepared material(C-dots) in 2ml of deionized water and contaminated water in parallel. After different absorption has been seen, for deionized water and contaminated water, we can distinguish while the material is degrading the pepticide or not. Lastly using ligh in different time of irradiation (20 min, 40 min, 60min, 80min and 100min) it will be degraded pollutant (treat water).

2.3. Photocatalytic Degradation of Methylene Blue

Modifications were made to the previous approach to evaluate the photocatalytic activity of the C-dots in degrading the MB dye under solar radiation [33,34]. Various experimental parameters, including dye concentration, irradiation period, reaction mixture pH, and catalyst dosage, were adjusted to optimize the outcomes. For each experiment, 20 mg of C-dots catalyst was dispersed in a 100 mL solution containing 10 mg/L of MB dye, with the pH adjusted to 8. The solution was then vigorously shaken for 30 minutes at approximately 600 rpm in the dark to establish an equilibrium of adsorption and desorption between the photocatalysts and the MB dye. To establish an adsorption/desorption equilibrium, the suspension was stirred in the dark at approximately 600 rpm for 30 minutes before solar exposure. The suspension was then subjected to direct sunlight for 120 minutes at the same stirring speed. At regular intervals of 20 minutes, 5 mL of the suspension was withdrawn and subjected to centrifugation at 6000 rpm for 15 minutes to remove the catalyst. The degree of degradation of the solution was analyzed using a UV-vis absorption spectrophotometer. **Equation 1** was utilized to determine the level of photocatalytic dye degradation.

$$\text{Percent of removal} = \frac{C_O - C_t}{C_O} \times 100 \quad (1)$$

Where, C_o (mg/L) is the initial MB dye concentration, C_t (mg/L) is the MB concentration at time t

3. Results and Discussion

3.1. Characterization

Researchers have employed TEM to investigate the size and morphology of C-dots. Based on the TEM images, the average size of the C-dots was determined to be 4.6 ± 1.5 nm. This means that the majority of the observed C-dots fell within the size range of 4 nm to 6 nm, with some variability around this average value. The size distribution is typically represented by a histogram, as shown in Figure 2, which indicates the frequency of C-dots at different size intervals. Moreover, the morphology of the C-dots was observed to be predominantly spherical, as indicated in Figure 2. This means that the C-dots exhibited a rounded shape resembling a sphere. Furthermore, the interplanar spacing of the C-dots was determined from the TEM images to be 0.284 nm. Interplanar spacing refers to the distance between adjacent crystal lattice planes within the C-dots. This value is inline with what has been reported in previous literature [32,35], suggesting that the internal structure of the C-dots aligns with the expected properties. Thus, TEM image C-dots findings contribute to a better understanding of the properties and potential applications of C-dots in various fields, including nanotechnology, materials science, and bioimaging [32].

 doi:10.20944/preprints202405.1578.v1

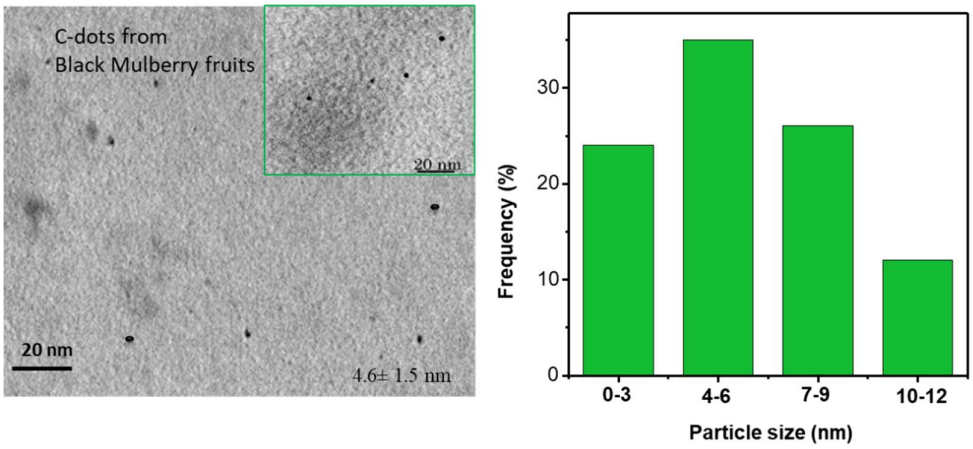

Figure 2. TEM image of C-dots fruit-derived Black mulberry.

UV-Vis spectroscopy experiments was conducted to analyze the optical properties of the C-dots (Figure 3(A). The observed absorption spectra exhibited distinctive peaks indicative of specific electronic transitions. Notably, a prominent peak at 350 nm was observed, which can be attributed to the n-π* electron transition of the carbonyl group. This transition arises due to the absorption of light in the ultraviolet region. Additionally, a smaller peak at 451 nm, as depicted in Figure 3(A), was observed and also assigned to n-π* electron transition, which can be both associated with the absorption of light in the vicinity of the C=O and C=N bonds. These bonds contribute to electronic transitions within the C-dots structure, resulting in the observed absorption at this wavelength range. The n-π* electron transition plays a significant role in the optical properties of carbon dots. This transition involves the excitation of an electron from the non-bonding (n) orbital to the anti-bonding (π*) orbital of the carbonyl group within the carbon dot structure and which can be insights into the chemical structure, conjugation, and functional groups present in the carbon dot system.

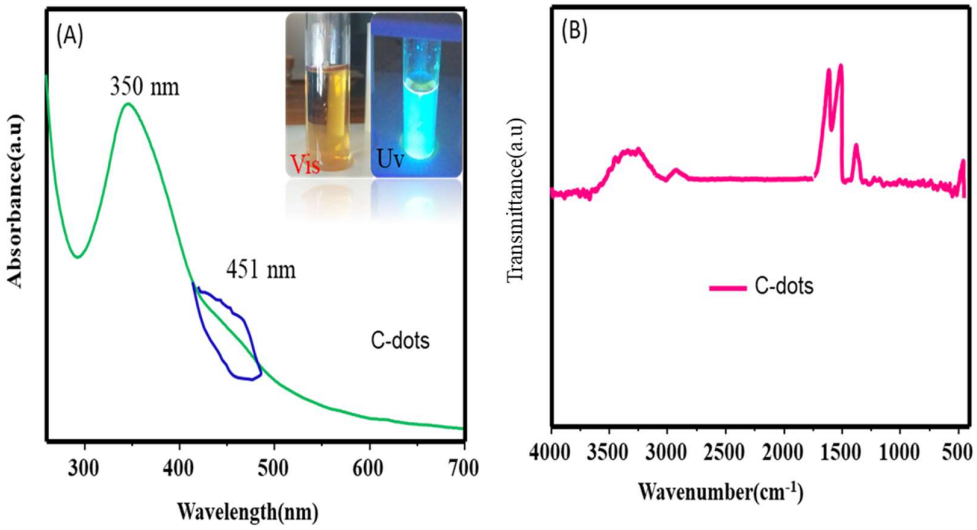

Figure 3. (A) Carbon dots's ultraviolet-visible light absorption spectrum from Black Mulberry fruits (B) Carbon dots's FTIR spectrum from Black Mulberry fruits.

FT-IR is a method used to analyze the molecular composition of a sample based on the absorption of infrared light. Five major bands observed in the FTIR spectrum of the C-dots rom Black Mulberry fruits (Figure 3(B). Each band corresponds to a specific vibration mode of different functional groups present in the C-dots rom Black Mulberry fruits. The bands appear at the following

 doi:10.20944/preprints202405.1578.v1

wavenumbers (in cm^{-1}) 3390 cm^{-1} band is attributed to the O-H vibration mode of carboxylic acid functional groups. Carboxylic acids contain a carboxyl group (-COOH), and the O-H bond in this group is responsible for this absorption. 2931 cm^{-1} band is assigned to the C-H (carbon-hydrogen) vibration mode of alkyl functional groups. Alkyl groups consist of carbon and hydrogen atoms bonded together, and the C-H bonds in these groups contribute to this absorption. 1662 cm^{-1} band is ascribed to the C=O vibration mode of carboxylic acid functional groups. The presence of a C=O bond in the carboxylic acid structure leads to this absorption. 1557 cm^{-1} band is assigned to the N−H/C=C vibration mode. It represents the combined vibrations of the N−H bond in amine functional groups and the C=C in the graphitic functional groups while 1390 cm^{-1} band corresponds to the C=C vibration mode of graphitic functional groups.

3.2. Photocatalytic Degradation Performance

Using C-dots catalysts under solar irradiation, the effects of starting dye concentration on the percentage of photocatalytic degradation were investigated, as shown in Figure 4. The catalyst dose was maintained at 300 mg/L throughout the experiment, although the dye (Methylene Blue, or MB) was initially added at 5, 10, and 15 mg/L. Following a 120-minute reaction time, the dyes' % clearance rates were determined (as illustrated in Figure 4). The findings demonstrated that when the concentration of MB dye rose, the breakdown rate of C-dots catalysts decreased. This can be explained by the fact that the dye's adsorption onto the catalyst's active sites approaches a balance as the dye concentration rises.

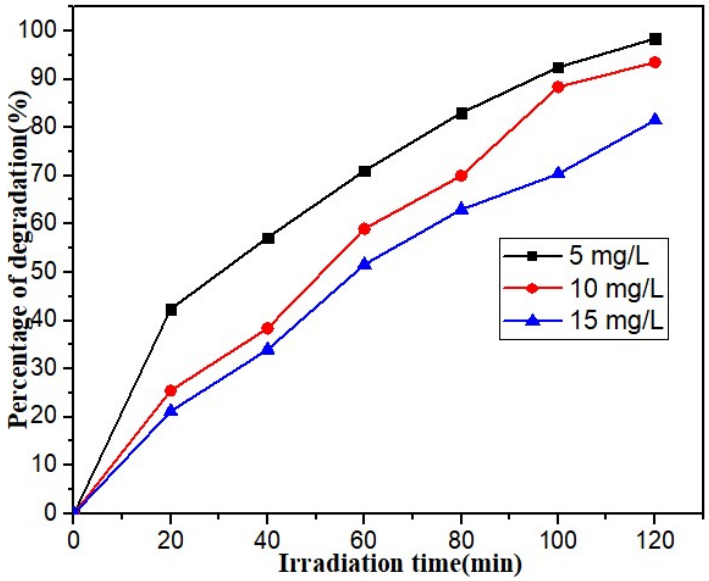

Figure 4. Effect of concentration of MB on photocatalytic degradations.

Dye molecules have the capacity to absorb large amounts of sunlight when they occupy these locations, which lowers the amount of light that reaches the catalyst. Because of this, there is less light penetration, which lowers the production of OH radicals—a crucial component in the process of photocatalytic degradation. The percentage of dye degradation is shown in Figure 4 of the study. After 120 minutes of irradiation, the dye's initial concentration of MB increased from 5 to 15 mg/L, resulting in a loss of 95.8% C-dots. In conclusion, the dye's concentration greatly affects the process of photocatalytic breakdown. Higher dye concentrations result in a decrease in the percentage degradation due to the increased adsorption of the dye on the catalyst's active sites, leading to reduced light penetration and OH radical formation. Because of the increased dye adsorption on the catalyst's active sites, which reduces light penetration and OH radical production, higher dye concentrations cause a drop in the percentage degradation.

 doi:10.20944/preprints202405.1578.v1

3.3. Photoluminsince Results

The fluorescence emission of C-dots (seen in Figure 5) is closely linked to their surface state, which includes factors such as surface functional groups and the degree of surface oxidation. Different functional groups on the C-Dots play a crucial role in determining the emission wavelengths. Higher content of C=O and carboxyl groups in the C-dots leads to higher emission efficiency. The full-color emission of C-dots is influenced more by functional groups rather than the degree of surface oxidation, as C-dots with similar oxygen content exhibit different colors. The exact underlying structure of C-dots fluorescence is not yet fully understood and requires further clarification due to the structural complexity of C-dots. Overall, excitation wavelengths and emission behavior in C-dots, the role of surface state and functional groups in emissions, and the need for further research to understand the fluorescence mechanism of C-dots.

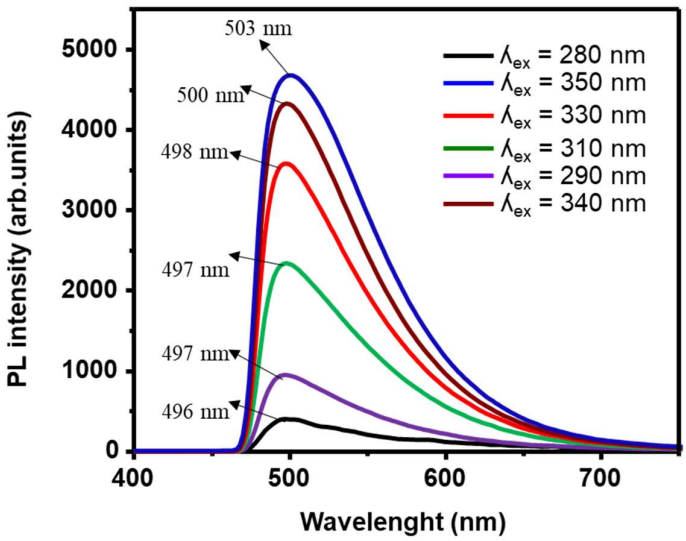

Figure 5. Carbon dot fluorescence emission spectrum at various excitation wavelengths.

Based on the information provided from Figure 6, the decay curves of C-dots (carbon dots) obtained at different excitation wavelengths (340 nm, 350 nm, 330 nm, and 310 nm). The decay curve refers to the rate at which the fluorescence intensity of the C-dots diminishes over time after excitation. Then among the mentioned excitation wavelengths, the decay curve at 350 nm exhibited the best performance, with a decay time of 6.73 ms. The decay time represents the characteristic time it takes for the fluorescence intensity to decrease to 1/e (approximately 36.8%) of its initial value. Typically, a shorter decay time indicates a faster decay rate and a less efficient fluorescence emission process. In this case, the C-dots excited at 350 nm showed the good life time, indicating a higher emission efficiency compared to the other excitation wavelengths tested (340 nm, 330 nm, and 310 nm.

 doi:10.20944/preprints202405.1578.v1

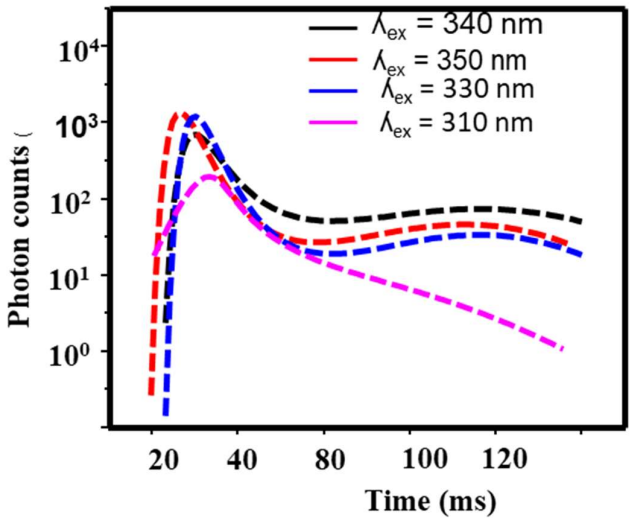

Figure 6. C-dot decay curves obtained at an excitation wavelength of each individual maximum intensity.

In the experiment, 0.2 mol% of C-dots were added to the water in order to reduce the pesticed in the water. The results of this experiment were presented in Figure 7, which presumably illustrates the decrease in pollutan concentration over time under visible light irradiation with a wavelength of 503 nm. According to the results shown in Figure 7, the pollutant concentration decreased significantly over a period of time under visible light irradiation. After 100 minutes of irradiation, the pollutan was almost fully degraded or eliminated at the concentration of 0.2 mol% of C-dots. This indicates that the C-dots exhibited strong photocatalytic activity, leading to the efficient degradation of the pollutant under visible light irradiation. The specific 0.2 mol% used in the experiment, along with the optimized concentration of C-dots, contributed to the successful degradation of the pollutant. Overall, the study demonstrates the potential of using C-dots as effective photocatalysts for the degradation of pollutant in the water, offering a promising approach for environmental remediation and the elimination of harmful substances.

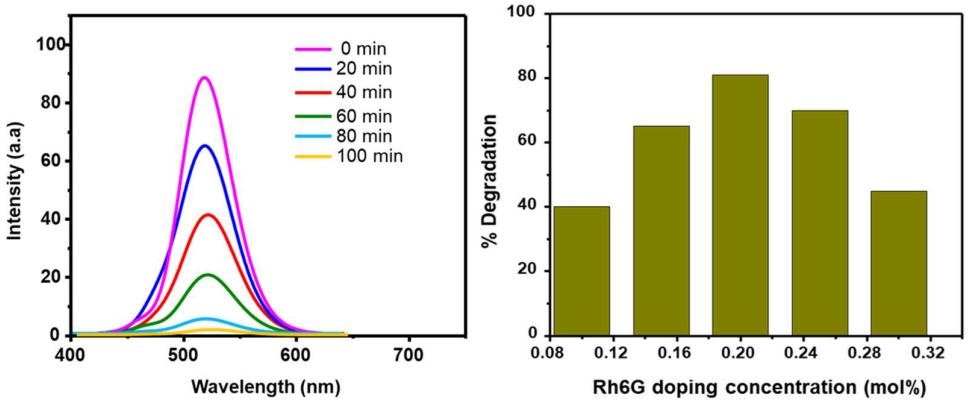

Figure 7. Photocatalytic degradation of pollutant using 0.2 mol% of C-dots.

4. Conclusions

In conclusion, the green synthesis of C-dots from black mulberry fruits involved a hydrothermal autoclave method using black mulberry fruit liquid and ethylenediamine. The resulting C-dots were characterized using TEM, which revealed an average size of 4.6 ± 1.5 nm and a predominantly spherical morphology. UV-Vis spectroscopy demonstrated distinctive absorption peaks at 350 nm and 451 nm, attributed to specific electronic transitions within the C-dots. FT-IR analysis identified functional groups such as carboxylic acids, alkyl groups, and graphitic functional groups in the C-

dots. The photoluminescence properties of the C-dots showed emission wavelengths influenced by surface functional groups. Decay curve analysis indicated that C-dots excited at 350 nm exhibited the best performance with a decay time of 6.73 ms. Furthermore, the C-dots demonstrated strong photocatalytic activity in the degradation of pollutants under visible light irradiation, as evidenced by the significant decrease in pollutant concentration over time. This research highlights the potential of C-dots as effective photocatalysts for environmental remediation and pollutant elimination.

Author Contributions: Conceptualization, H.F.E. and A.A.T methodology, F.B.D.; validation, H.F.E., A.A.Tand F.B.D formal analysis, H.F.T.; investigation, F.B.D.; resources, H.F.E, writ-ing—original draft preparation, A.A.T.; writing—review and editing, F.B.D; visualization, F.B.D.; supervision, F.B.D; project administration, F.B.D; funding acquisition. All authors have read and agreed to the published version of the manuscript.".

Funding: This research did not receive any specific grant from public funding agencies. This work is supported by the WSU (with ESKOM project).

Data Availability Statement: The data used is confidently included in this manuscript.

Acknowledgments: The authors are grateful to Walter Sisulu University (WSU) for its support.

Conflicts of Interest: The authors declare no conflicts of interest.

References

1. Zhou, Z.; Shen, Y.; Li, Y.; Liu, A.; Liu, S.; Zhang, Y. Chemical cleavage of layered carbon nitride with enhanced photoluminescent performances and photoconduction. *ACS nano* **2015**, *9*, 12480-12487.
2. Xiao, L.; Wang, Y.; Huang, Y.; Wong, T.; Sun, H. Self-trapped exciton emission from carbon dots investigated by polarization anisotropy of photoluminescence and photoexcitation. *Nanoscale* **2017**, *9*, 12637-12646.
3. Li, Y.; Miao, P.; Zhou, W.; Gong, X.; Zhao, X. N-doped carbon-dots for luminescent solar concentrators. *Journal of Materials Chemistry A* **2017**, *5*, 21452-21459.
4. Hola, K.; Zhang, Y.; Wang, Y.; Giannelis, E.P.; Zboril, R.; Rogach, A.L. Carbon dots—Emerging light emitters for bioimaging, cancer therapy and optoelectronics. *Nano Today* **2014**, *9*, 590-603.
5. Stepanidenko, E.A.; Ushakova, E.V.; Fedorov, A.V.; Rogach, A.L. Applications of carbon dots in optoelectronics. *Nanomaterials* **2021**, *11*, 364.
6. Wang, B.; Lu, S. The light of carbon dots: From mechanism to applications. *Matter* **2022**, *5*, 110-149.
7. Kamiloglu, S.; Serali, O.; Unal, N.; Capanoglu, E. Antioxidant activity and polyphenol composition of black mulberry (morus nigra l.) products. *Journal of Berry Research* **2013**, *3*, 41-51.
8. Luo, W.-K.; Zhang, L.-L.; Yang, Z.-Y.; Guo, X.-H.; Wu, Y.; Zhang, W.; Luo, J.-K.; Tang, T.; Wang, Y. Herbal medicine derived carbon dots: Synthesis and applications in therapeutics, bioimaging and sensing. *Journal of Nanobiotechnology* **2021**, *19*, 1-30.
9. Kanwal, A.; Bibi, N.; Hyder, S.; Muhammad, A.; Ren, H.; Liu, J.; Lei, Z. Recent advances in green carbon dots (2015–2022): Synthesis, metal ion sensing, and biological applications. *Beilstein Journal of Nanotechnology* **2022**, *13*, 1068-1107.
10. Umar, M.; Aziz, H.A. Photocatalytic degradation of organic pollutants in water. *Organic pollutants-monitoring, risk and treatment* **2013**, *8*, 196-197.
11. Ajith, M.; Aswathi, M.; Priyadarshini, E.; Rajamani, P. Recent innovations of nanotechnology in water treatment: A comprehensive review. *Bioresource Technology* **2021**, *342*, 126000.
12. Anju, A.; Ravi S, P.; Bechan, S. Water pollution with special reference to pesticide contamination in india. *Journal of Water Resource and Protection* **2010**, *2010*.
13. Akhtar, N.; Syakir Ishak, M.I.; Bhawani, S.A.; Umar, K. Various natural and anthropogenic factors responsible for water quality degradation: A review. *Water* **2021**, *13*, 2660.
14. Bhosale, T.; Kuldeep, A.; Pawar, S.; Shirke, B.; Garadkar, K. Photocatalytic degradation of methyl orange by eu doped sno 2 nanoparticles. *Journal of Materials Science: Materials in Electronics* **2019**, *30*, 18927-18935.
15. Georgakilas, V.; Perman, J.A.; Tucek, J.; Zboril, R. Broad family of carbon nanoallotropes: Classification, chemistry, and applications of fullerenes, carbon dots, nanotubes, graphene, nanodiamonds, and combined superstructures. *Chemical reviews* **2015**, *115*, 4744-4822.
16. Barman, M.K.; Patra, A. Current status and prospects on chemical structure driven photoluminescence behaviour of carbon dots. *Journal of Photochemistry and Photobiology C: Photochemistry Reviews* **2018**, *37*, 1-22.
17. Sharma, A.; Das, J. Small molecules derived carbon dots: Synthesis and applications in sensing, catalysis, imaging, and biomedicine. *Journal of nanobiotechnology* **2019**, *17*, 1-24.
18. Özkara, A.; Akyıl, D.; Konuk, M. Pesticides, environmental pollution, and health. In *Environmental health risk-hazardous factors to living species*, IntechOpen: 2016.

 doi:10.20944/preprints202405.1578.v1

19. Chauhan, D.S.; Quraishi, M.; Verma, C. Carbon nanodots: Recent advances in synthesis and applications. *Carbon Letters* **2022**, *32*, 1603-1629.
20. Mansuriya, B.D.; Altintas, Z. Carbon dots: Classification, properties, synthesis, characterization, and applications in health care—An updated review (2018–2021). *Nanomaterials* **2021**, *11*, 2525.
21. Cailotto, S.; Massari, D.; Gigli, M.; Campalani, C.; Bonini, M.; You, S.; Vomiero, A.; Selva, M.; Perosa, A.; Crestini, C. N-doped carbon dot hydrogels from brewing waste for photocatalytic wastewater treatment. *ACS omega* **2022**, *7*, 4052-4061.
22. Patial, S.; Sudhaik, A.; Chandel, N.; Ahamad, T.; Raizada, P.; Singh, P.; Chaukura, N.; Selvasembian, R. A review on carbon quantum dots modified g-c3n4-based photocatalysts and potential application in wastewater treatment. *Applied Sciences* **2022**, *12*, 11286.
23. Gautam, S.; Agrawal, H.; Thakur, M.; Akbari, A.; Sharda, H.; Kaur, R.; Amini, M. Metal oxides and metal organic frameworks for the photocatalytic degradation: A review. *Journal of Environmental Chemical Engineering* **2020**, *8*, 103726.
24. Zhang, X.; Kamali, M.; Zhang, S.; Yu, X.; Appels, L.; Cabooter, D.; Dewil, R. Photo-assisted (waste) water treatment technologies—A scientometric-based critical review. *Desalination* **2022**, *538*, 115905.
25. Gudimella, K.K.; Appidi, T.; Wu, H.-F.; Battula, V.; Jogdand, A.; Rengan, A.K.; Gedda, G. Sand bath assisted green synthesis of carbon dots from citrus fruit peels for free radical scavenging and cell imaging. *Colloids and Surfaces B: Biointerfaces* **2021**, *197*, 111362.
26. Gutiérrez-Cruz, A.; Ruiz-Hernández, A.R.; Vega-Clemente, J.F.; Luna-Gazcón, D.G.; Campos-Delgado, J. A review of top-down and bottom-up synthesis methods for the production of graphene, graphene oxide and reduced graphene oxide. *Journal of Materials Science* **2022**, *57*, 14543-14578.
27. El-Shafey, A.M. Carbon dots: Discovery, structure, fluorescent properties, and applications. *Green Processing and Synthesis* **2021**, *10*, 134-156.
28. Nemera, D.J.; Etefa, H.F.; Kumar, V.; Dejene, F.B. Hybridization of nickel oxide nanoparticles with carbon dots and its application for antibacterial activities. *Luminescence* **2022**, *37*, 965-970.
29. Manzoor, S.; Dar, A.H.; Dash, K.K.; Pandey, V.K.; Srivastava, S.; Bashir, I.; Khan, S.A. Carbon dots applications for development of sustainable technologies for food safety: A comprehensive review. *Applied Food Research* **2023**, 100263.
30. Shanker, U.; Hussain, C.M.; Rani, M. *Green functionalized nanomaterials for environmental applications*. Elsevier: 2021.
31. Etefa, H.F.; Nemera, D.J.; Dejene, F.B. Green synthesis of nickel oxide nps incorporating carbon dots for antimicrobial activities. *ACS Omega* **2023**.
32. Etefa, H.F.; Kumar, V.; Dejene, F.B.; Efa, M.T.; Jule, L.T. Modification of flexible electrodes for p-type (nickel oxide) dye-sensitized solar cell performance based on the cellulose nanofiber film. *ACS omega* **2023**, *8*, 15249-15258.
33. Alzahrani, E.A.; Nabi, A.; Kamli, M.R.; Albukhari, S.M.; Althabaiti, S.A.; Al-Harbi, S.A.; Khan, I.; Malik, M.A. Facile green synthesis of zno nps and plasmonic ag-supported zno nanocomposite for photocatalytic degradation of methylene blue. *Water* **2023**, *15*, 384.
34. Peng, G.; Chou, N.-N.; Lin, Y.-S.; Yang, C.-F.; Meen, T.-H. Comparison of the degradation effect of methylene blue for zno nanorods synthesized on silicon and indium tin oxide substrates. *Materials* **2023**, *16*, 4275.
35. Etefa, H.F.; Imae, T.; Yanagida, M. Enhanced photosensitization by carbon dots co-adsorbing with dye on p-type semiconductor (nickel oxide) solar cells. *ACS applied materials & interfaces* **2020**, *12*, 18596-18608.